inhibits four PI3K isoforms potently, with IC_{50} values of 16, 44, 5, 49 nM for PI3Kα, β, δ, and γ, respectively.[21] (see Fig. 2A) Docking analysis by using the crystal structure of PI3Kγ-LY294002 as a model suggested that ZSTK474 binds with PI3K in the ATP-binding pocket. Lineweaver–Burk plots also indicated that ZSTK474 inhibits PI3K by competing with ATP for a common binding site.[21] In vitro, ZSTK474 inhibited the growth of 39 human cancer cell lines with a mean GI50 value of 0.32 μM,[17] and blocked cell cycle progression at G0/G1 phase in various human cancer cells without obvious induction of apoptosis.[17,22] Moreover, ZSTK474 displayed a potent anti-angiogenic effect via two mechanisms: (i) inhibition of HIF-1α expression and VEGF production in cancer cells, and (ii) blockage in the proliferation, migration, and tube formation of HUVECs (human umbilical vein endothelial cells). (see Fig. 2B).[23] Oral administration of ZSTK474 indicated obvious in vivo antitumor efficacy against various cancer xenografts (see Fig. 2C) at both early and advanced stages, without any obvious toxicity.[6,22,23] Given the favorable preclinical antitumor effect and safety, an investigational new drug application for ZSTK474 has been approved by the US FDA and the compound is in phase I clinical trials.[4]

We also investigated the application of JFCR39 for prediction of target specificity by using several PI3K inhibitors. In addition to four class I PI3K isoforms, we determined the activities of PI3K inhibitors ZSTK474, GDC-0941 and NVP-BEZ235 against the kinases with a related structure or function (PI3K superfamily[12]): PI3KC2α and PI3KC2β (class II PI3K), vacuolar protein sorting 34 (Vps34, Class III PI3K), mTOR and DNA-dependent protein kinase (DNA-PK) (Class IV PI3K), and phosphatidylinositol 4-kinase (PI4K). The IC_{50} values were calculated and used to plot the inhibition profiles of each inhibitor. As shown in Figure 3A, ZSTK474 and GDC-0941 were found to be class I PI3K-specific PI3K inhibitors, by displaying selectivity over mTOR, DNA-PK, and other PI3K superfamily members. In contrast, NVP-BEZ235 showed more potent activity against mTOR and DNA-PK than against class I PI3Ks,[12,24] suggesting the low selectivity for class I PI3K inhibition. We then compared the JFCR39 fingerprints of the three PI3K inhibitors (see Fig. 3B). Interestingly, ZSTK474 showed a more similar fingerprint with GDC-0941 ($r = 0.863$), compared to that with BEZ235 ($r = 0.67$),[12] consistent with our biochemical assay results regarding inhibition of kinases belonging to the PI3K superfamily. Taken together, these results suggest that JFCR39 can be used to predict specificity for the molecular target of a certain antitumor agent. Furthermore, baicalein, a natural-product PI3K inhibitor we discovered from our SCADS library, also exhibits a different fingerprint to that of ZSTK474.[25] Baicalein is a flavonoid that inhibits various enzymes including 12-lipoxygenase.[25]

We recently reported a cluster analysis of 67 anticancer compounds, including PI3K/Akt/mTOR inhibitors, Mek inhibitors, and other conventional anticancer drugs, by use of their LogGI50s for each cell line of JFCR39,[6] further supported that JFCR39 could identify anticancer compounds with various targets.

4. Conclusion

As a bioinformatics system, JFCR39 has made a significant contribution to the discovery and development of anticancer drugs. In particular, since the JFCR39 screening system became a key part of the program of Screening Committee of Anticancer Drugs (SCADS, funded by the Ministry of Education, Science and Culture) of Japan,[25] JFCR39 has become a well known platform for the discovery of molecular-targeted anticancer drugs in Japan. Information from the JFCR39 system has facilitated the selection of many compounds for active development as anticancer drug candidates, some of which have entered clinical trials (e.g., ZSTK474).[4,14] The first molecular-targeted anticancer drug to be identified by JFCR39 is anticipated to enter the market in the near future.

Acknowledgments

We thank Dr. R.H. Shoemaker and Dr. K.D. Paull for discussion on the establishment of the JFCR39 anticancer drug screening system. This work was supported by a grant from The Natural Science Foundation of Tianjin; a grant from '211' project of Tianjin Medical University; a Grant from the 973 program (2011CB933100); a Grant from the National Institute of Biomedical Innovation, Japan to T. Yamori (05-13); a grants-in-aid of the Priority Area 'Cancer' from the Ministry of Education, Culture, Sports, Science, and Technology of Japan to T. Yamori (20015048); a grants-in-aid for Scientific Research (A) from Japan Society for the Promotion of Science to T. Yamori (22240092); a Grant from Kobayashi institute for innovative cancer chemotherapy.

References and notes

1. Sharma, S. V.; Haber, D. A.; Settleman, J. *Nature Rev.* **2010**, *10*, 241.
2. O'Brien, C.; Wallin, J. J.; Sampath, D.; GuhaThakurta, D.; Savage, H.; Punnoose, E. A.; Guan, J.; Berry, L.; Prior, W. W.; Amler, L. C.; Belvin, M.; Friedman, L. S.; Lackner, M. R. *Clin. Cancer Res.* **2010**, *16*, 3670.
3. Shoemaker, R. H. *Nature Rev.* **2006**, *6*, 813.
4. Kong, D. X.; Yamori, T. *Acta Pharmacol. Sin.* **2010**, *31*, 1189.
5. Yamori, T. *Cancer Chemother. Pharmacol.* **2003**, *52*(Suppl 1), S74.
6. Dan, S. O. M.; Seki, M.; Yamazaki, K.; Sugita, H.; Okui, M.; Mukai, Y.; Nishimura, H. *Cancer Res.* **2010**, *70*, 4982.
7. Skehan, P.; Storeng, R.; Scudiero, D.; Monks, A.; McMahon, J.; Vistica, D.; Warren, J. T.; Bokesch, H.; Kenney, S.; Boyd, M. R. *J. Natl. Cancer Inst.* **1990**, *82*, 1107.
8. Nakatsu, N.; Nakamura, T.; Yamazaki, K.; Sadahiro, S.; Makuuchi, H.; Kanno, J.; Yamori, T. *Mol. Pharmacol.* **2007**, *72*, 1171.
9. Yamori, T.; Matsunaga, A.; Sato, S.; Yamazaki, K.; Komi, A.; Ishizu, K.; Mita, I.; Edatsugi, H.; Matsuba, Y.; Takezawa, K.; Nakanishi, O.; Kohno, H.; Nakajima, Y.; Komatsu, H.; Andoh, T.; Tsuruo, T. *Cancer Res.* **1999**, *59*, 4042.
10. Monks, A.; Scudiero, D.; Skehan, P.; Shoemaker, R.; Paull, K.; Vistica, D.; Hose, C.; Langley, J.; Cronise, P.; Vaigro-Wolff, A., et al *J. Natl. Cancer Inst.* **1991**, *83*, 757.
11. Paull, K. D.; Shoemaker, R. H.; Hodes, L.; Monks, A.; Scudiero, D. A.; Rubinstein, L.; Plowman, J.; Boyd, M. R. *J. Natl. Cancer Inst.* **1989**, *81*, 1088.
12. Kong, D.; Dan, S.; Yamazaki, K.; Yamori, T. *Eur. J. Cancer* **2010**, *46*, 1111.
13. Naasani, I.; Seimiya, H.; Yamori, T.; Tsuruo, T. *Cancer Res.* **1999**, *59*, 4004.
14. Mizui, Y.; Sakai, T.; Iwata, M.; Uenaka, T.; Okamoto, K.; Shimizu, H.; Yamori, T.; Yoshimatsu, K.; Asada, M. *J. Antibiot.* **2004**, *57*, 188.
15. Kotake, Y.; Sagane, K.; Owa, T.; Mimori-Kiyosue, Y.; Shimizu, H.; Uesugi, M.; Ishihama, Y.; Iwata, M.; Mizui, Y. *Nat. Chem. Biol.* **2007**, *3*, 570.
16. Yaguchi, S.; Izumisawa, Y.; Sato, M.; Nakagane, T.; Koshimizu, I.; Sakita, K.; Kato, M.; Yoshioka, K.; Sakato, M.; Kawashima, S. *Biol. Pharm. Bull.* **1997**, *20*, 698.
17. Yaguchi, S.; Fukui, Y.; Koshimizu, I.; Yoshimi, H.; Matsuno, T.; Gouda, H.; Hirono, S.; Yamazaki, K.; Yamori, T. *J. Natl. Cancer Inst.* **2006**, *98*, 545.
18. Kong, D.; Yamori, T. *Cancer Sci.* **2008**, *99*, 1734.
19. Toker, A.; Cantley, L. C. *Nature* **1997**, *387*, 673.
20. Kong, D.; Yamori, T. *Curr. Med. Chem.* **2009**, *16*, 2839.
21. Kong, D.; Yamori, T. *Cancer Sci.* **2007**, *98*, 1638.
22. Dan, S.; Yoshimi, H.; Okamura, M.; Mukai, Y.; Yamori, T. *Biochem. Biophys. Res. Commun.* **2009**, *379*, 104.
23. Kong, D.; Okamura, M.; Yoshimi, H.; Yamori, T. *Eur. J. Cancer* **2009**, *45*, 857.
24. Kong, D.; Yaguchi, S.; Yamori, T. *Biol. Pharm. Bull.* **2009**, *32*, 297.
25. Kong, D.; Yamazaki, K.; Yamori, T. *Biol. Pharm. Bull.* **2010**, *33*, 1600.

Cancer Science
The official journal of the Japanese Cancer Association
JCA

Effectiveness of combined treatment using X-rays and a phosphoinositide 3-kinase inhibitor, ZSTK474, on proliferation of HeLa cells *in vitro* and *in vivo*

Kazunori Anzai,[1,2] Emiko Sekine-Suzuki,[1] Megumi Ueno,[1] Mutsumi Okamura,[3] Hisashi Yoshimi,[3,4] Shingo Dan,[3] Shin-ichi Yaguchi,[3,4] Jumpei Enami,[4] Takao Yamori[3,5] and Ryuichi Okayasu[1,5]

[1]Heavy-ion Radiobiology Research Group, National Institute of Radiological Sciences, Chiba; [2]Nihon Pharmaceutical University, Saitama; [3]Division of Molecular Pharmacology, Cancer Chemotherapy Center, Japanese Foundation for Cancer Research, Tokyo; [4]Central Research Laboratory, Zenyaku Kogyo Co., Tokyo, Japan

(Received January 5, 2011/Revised February 15, 2011/Accepted February 21, 2011/Accepted manuscript online February 26, 2011/Article first published online April 4, 2011)

ZSTK474 is a novel orally applicable phosphoinositide 3-kinase-specific inhibitor that strongly inhibits cancer cell proliferation. To further explore the antitumor effect of ZSTK474 for future clinical usage, we studied its combined effects with radiation. The proliferation of HeLa cells was inhibited by treatment with X-rays alone or ZSTK474 alone. Combination treatment using X-rays then ZSTK474 given orally for 8 days, starting 24 h post-irradiation, significantly enhanced cell growth inhibition. The combined effect was also observed for clonogenic survival with continuous ZSTK474 treatment. Western blot analysis showed enhanced phosphorylation of Akt and GSK-3β by X-irradiation, whereas phosphorylation was inhibited by ZSTK474 treatment alone. Treatment with ZSTK474 after X-irradiation also inhibited phosphorylation, and remarkably inhibited xenograft tumor growth. Combined treatment with X-rays and ZSTK474 has greater therapeutic potential than radiation or drug therapy alone, both *in vitro* and *in vivo*. (*Cancer Sci* 2011; 102: 1176–1180)

Phosphoinositide 3-kinases (PI3Ks) are a family of lipid kinase that phosphorylates the 3-hydroxyl group of the inositol ring of phosphoinositides.[1] As PI3Ks have been shown to be important targets in cancer therapy, development of PI3K inhibitors has attracted attention from both academic and industrial researchers. Recently, several novel PI3K inhibitors have been developed and some of them are now undergoing clinical trial.[2]

Among the novel PI3K inhibitors, ZSTK474 has unique properties.[1,3–6] ZSTK474 is a pan-PI3K inhibitor: it inhibits all four PI3K isoforms in an ATP-competitive manner. Among all of the PI3K isoforms, PI3Kδ was inhibited most potently by ZSTK474. PI3K-related kinases are a group of protein kinases with a catalytic core structure similar to PI3K, but they lack the lipid kinase activity. This group includes mTOR, DNA-PK, ATM, and ATR proteins, of which the latter three are known to be involved in DNA damage-related responses. The inhibition activity of ZSTK474 against DNA-PK and mTOR was determined, and was shown to be far weaker compared with that observed against PI3K. These results indicate that ZSTK474 was the most specific agent among these PI3K inhibitors.[1,4,6] The inhibition selectivity of ZSTK474 for PI3K over DNA-PK was significantly higher than other PI3K inhibitors such as NVP-BEZ235, PI-103, and LY294002.[6] *In vitro*, ZSTK474 induced marked G_0/G_1 arrest in various human cancer cells without any obvious apoptosis.[3,5] This pan-PI3K inhibitor, given orally, showed potent *in vivo* antitumor efficacy on cancer xenografts at both early and advanced stages, without obvious toxicity being observed.[3]

ZSTK474 strongly inhibited tumor growth. Thus, to consider the clinical usage of ZSTK474, its combination with another therapy is a practical choice. In single drug therapy, the use of multiple agents, such as chemotherapeutic drugs and radiation, increases effectiveness and potency in clinical cancer therapy. Radiation can be used as an agent to increase the anticancer effect of ZSTK474, as ZSTK474 effectively inhibits the downstream of the PI3K pathway.

In general, the combination of chemotherapy and radiotherapy can be classified into three categories based on the time sequence of the treatments: neoadjuvant (chemotherapy before radiotherapy); concurrent; and adjuvant (chemotherapy after radiotherapy) chemo-radiotherapy. The time sequence of the treatments usually affects the results. It is known that the sensitivity of cells to radiation depends on the cell cycle phases.[7] The cells are most sensitive to low linear energy transfer (LET) ionizing radiation when irradiated at G_2/M phase and are most resistant when irradiated at late S phase. Other phases, such as G_1 and early S, show intermediate sensitivity. As ZSTK474 induces arrest in the G_0/G_1 phase of the cell cycle, where radiation sensitivity is not the highest, ZSTK474 was not used in this study in the typical manner of radiation sensitizers. In addition, ZSTK474 is a specific PI3K inhibitor, and it showed weaker inhibitory activity against DNA-PKcs, which is thought to be essential for the double strand break (DSB) repair process after radiation exposure.

We then examined the time sequence where ZSTK474 was applied not immediately, but much later after irradiation. In this study, significant combination effects of X-rays and ZSTK474 were observed both *in vitro* and *in vivo*.

Materials and Methods

Chemicals. ZSTK474 was synthesized in the Central Research Laboratory, Zenyaku Kogyo Co. (Tokyo, Japan). For *in vitro* studies, ZSTK474 was dissolved in DMSO. For animal experiments, ZSTK474 was suspended in 5% hydroxypropyl cellulose in water as a solid dispersion form.[3]

Animals. All animal experiments were carried out at the National Institute of Radiological Sciences (NIRS; Chiba, Japan), conformed to institutional guidelines, and were approved by the Institutional Animal Care and Use Committee of NIRS. Male nude mice (BALB/c-nu/nu) were obtained at 6 weeks of age from CLEA Japan (Tokyo, Japan). The mice were housed in a temperature- and humidity-controlled room at 23 ± 1°C and 55 ± 5%, respectively, and maintained on a 12:12 light:dark cycle. The mice were kept five per cage. They received acidified water and diet (MB-1; Funabashi Farm, Funabashi, Japan) *ad libitum* during the experimental period.

[5]To whom correspondence should be addressed.
E-mail: yamori@jfcr.or.jp; rokayasu@nirs.go.jp

doi: 10.1111/j.1349-7006.2011.01916.x

Cell cultures. The HeLa cell line (human cervix epithelium carcinoma) was obtained from the Cell Resource Center for Biomedical Research, Tohoku University (Sendai, Japan). The cells were grown in DMEM (Sigma-Aldrich, Tokyo, Japan) supplemented with 10% FBS and antibiotic–antimycotic (Gibco-Invitrogen, Tokyo, Japan) at 37°C with 5% CO_2.

X-irradiation. HeLa cells in dishes were X-irradiated with a Shimadzu Pantak HF-320 at a dose rate of 0.95 Gy/min (200 kVp, 20 mA, 0.5 mm Al + 0.5 mm Cu filter). For the irradiation of mice, nude mice bearing xenograft tumors at the right hind leg were placed on a Lucite plate and the tumors were X-irradiated at a dose rate of 1.27 Gy/min with the Shimadzu Pantak HF-320 (200 kVp, 20 mA, 0.5 mm Al + 0.5 mm Cu filter).

Cell viability assay. HeLa cells in 60 mm dishes were prepared at various cell densities 1 day before X-irradiation. One day later, the cells were X-irradiated (2 Gy) at room temperature (day 0). At 24 h after X-irradiation (day 1), the cells were exposed to ZSTK474 (1 μM). When counting cell numbers, the medium in the dish was transferred to 15 mL plastic tubes to count the number of dead cells. The remaining cells attached to the dishes were washed with PBS and the PBS was transferred to the plastic tubes to combine with the medium. The cells on the dishes were trypsinized for 5 min at 37°C and the cell suspensions were combined with the medium in the plastic tubes. The combined suspensions were centrifuged at 110*g* for 5 min at 4°C with a M160-IV centrifuge (Sakuma, Tokyo, Japan). The pellet was suspended in 0.5 mL PBS and the number of cells was counted under a microscope (Olympus IX-70 Fluorescence microscope; Olympus, Tokyo, Japan) on days 0, 1, 2, 3, 4, 5, and 8. The relative growth rates were calculated based on the number of cells counted at the time of X-irradiation (day 0). Each point on the cell growth curve represents the mean and the standard deviation from four samples.

Clonogenic cell survival assay. The clonogenic cell survival rate was determined by the colony-forming assay. Immediately after irradiation, cells were washed with PBS, trypsinized, diluted, and seeded in 60-mm dishes at various cell densities. At 24 h after irradiation, the cells were exposed to ZSTK474 for 24 h, then the medium was changed to ZSTK474-free medium and incubated at 37°C for 2 weeks (transient exposure). Alternatively, the cells were exposed to ZSTK474 at 24 h after irradiation, then continuously exposed for 2 weeks during the incubation (continuous exposure). After 2 weeks of incubation, colonies were stained with crystal violet dissolved in methanol. Colonies containing more than 50 cells were counted directly by eye or by a scanner. NIH Image software (Image J, http://rsb.info.nih.gov/ij/) was used for the analysis of number and area of colony. The surviving fraction was calculated based on the plating efficiency determined from the control (no X-irradiation, drug only). Each point on the survival curve represents the mean surviving fraction from three dishes. Clonogenic survival curves are representative of independent triplicate experiments.

Western blot analysis. Preparation of samples for Western blot analysis was carried out according to the following method.[3,8] The sample dishes were frozen in liquid nitrogen, and the cells were lysed in a buffer containing 10 mM Tris–HCl at pH 7.4, 50 mM NaCl, 50 mM NaF, 30 mM sodium pyrophosphate, 50 mM sodium orthovanadate, 5 mM EDTA, 1 mM PMSF, 0.5% Nonidet P-40, 0.1% SDS, and one complete protease inhibitor cocktail tablet (Roche Diagnostics, Tokyo, Japan). Proteins in cell extracts were separated by SDS-PAGE) at a constant voltage (150 V), then electrotransferred onto nitrocellulose membranes (Invitrogen, Tokyo, Japan) at 30 V. The membranes were incubated with a primary antibody overnight at 4°C, and a secondary antibody for 1 h at 37°C. Finally, the blots were visualized by the enhanced chemiluminescence method (GE Healthcare, Tokyo, Japan) according to the manufacturer's instructions. Primary antibodies used for immunoblotting were as follows: rabbit polyclonal antibodies for Akt, phosphorylated Akt (phosphorylated residue Ser473), phosphorylated Akt (phosphorylated residue Thr308), phosphorylated glycogen synthase kinase 3β (GSK-3β, phosphorylated residue Ser9), and β-actin. Secondary antibodies used were goat polyclonal anti-rabbit IgG-HRP (Santa Cruz Biotechnology, Santa Cruz, CA, USA).

***In vivo* study for tumor growth in xenograft model.** Nude mice (BALB/c-nu/nu, 8-week-old) were injected s.c. with 10^6 HeLa cells in 100 μL PBS. Approximately 2 weeks after inoculation, when the tumors had reached an average volume of 150 mm^3, the mice were divided into four groups: group 1, control ($n = 6 + 2$); group 2, X-rays ($n = 6 + 2$); group 3, ZSTK474 ($n = 6 + 2$); and group 4, X-rays + ZSTK474 ($n = 6 + 2$). On day 0, the tumors on the right hind legs of mice were X-irradiated at 8 Gy (groups 2 and 4). 24 hours after 8 Gy irradiation on the tumor, the mice began an oral inoculation regime of 100 mg/kg ZSTK474, given 11 times in 15 days, every day from day 1 to day 15 except for days 3, 4, 10, and 11. Body weight of the mice was measured before each dose of ZSTK474. ZSTK474 was suspended in 5% hydroxypropyl methylcellulose in water as a solid dispersion form at just before use. The size of palpable tumors in the mice ($n = 6$ per group) was measured with calipers every 2–4 days. The tumor volume (V) was calculated as V (mm^3) = length (mm) × width $(mm)^2/2$. Animals were killed when tumors exceeded 1000 mm^3 in size or became severely necrotic.

Immunohistochemical analysis. Two mice from each group on day 2 and two mice from groups 2, 3, and 4 on day 15 were used for immunohistochemical (IHC) analysis of tumors.[5] For these experiments, each group involved an additional two mice (total of eight mice). For IHC analysis, tumor tissues were fixed in 10% neutral formalin and embedded in paraffin. Tissue sections (4 μm) were deparaffinized in xylene and rehydrated through graded ethanol solutions. Antigen retrieval was carried out using 10 mM Tris–EDTA buffer (pH 9.0). Specific antibody against phosphorylated Akt (Ser473) (Cell Signaling Technology, Danvers, MA, USA) were used for hybridization and the bound antibodies were visualized by a Dako EnVision kit (Dako Cytomation, Glostrup, Denmark) containing a secondary HRP-conjugated anti-rabbit polymer antibody complex. Sections were counterstained with Mayer's hematoxylin.

Statistical analysis. The statistical analysis of mean values was carried out using Student's *t*-test. Differences with a *P*-value <0.05 were considered statistically significant. Data shown are the mean and SD.

Results

Effect of combined treatment on *in vitro* HeLa cell proliferation. Effects of treatment with X-rays alone, ZSTK474 alone, or the combination of both agents on HeLa cell proliferation were examined *in vitro*. The cells were irradiated with X-rays at 2 Gy (day 0) and 24 h later (day 1) treated with 1 μM ZSTK474 dissolved in DMSO. The number of cells was counted on days 1, 2, 3, 4, 5, and 8. As shown in Figure 1, the cell proliferation was inhibited by the treatment with X-rays alone, ZSTK474 alone, and the combination of both agents. The inhibition of cell proliferation by X-irradiation alone was 52% and 58% on days 4 and 8, respectively. The inhibition by ZSTK474 alone was 55% and 69% on days 4 and 8, respectively. Interestingly, a dramatic inhibitory effect was observed on day 8 of the combination treatment. The inhibition by treatment using X-rays and ZSTK474 was 76% and 91% on days 4 and 8, respectively.

Effect of combined treatment of X-rays and ZSTK474 on clonogenic cell survival. Clonogenic cell survival was examined for HeLa cells by colony-forming assay. Figure 2(A) shows a representative result of clonogenic cell survival in three independent experiments for transient (24 h) ZSTK474

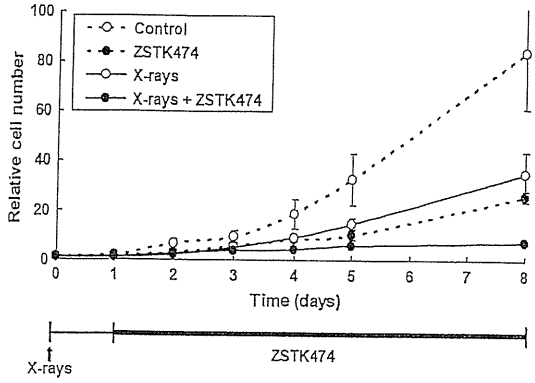

Fig. 1. Effect of treatment with X-rays alone, ZSTK474 alone, or a combination of both agents on the proliferation of HeLa cells. The cells were prepared in 60-mm dishes at various cell densities 1 day before X-irradiation. For treatment with X-rays alone, the cells were X-irradiated (2 Gy) 1 day later (day 0). For treatment with ZSTK474 alone, 2 days later (day 1), the cells were exposed to 1 μM ZSTK474. For X-rays + ZSTK474, the cells were treated with 1 μM ZSTK474 24-h after 2 Gy X-irradiation. The number of cells was counted on days 0, 1, 2, 3, 4, 5, and 8 under a microscope. The relative values of the number of the cells based on the number on the day of X-irradiation (day 0) are shown.

treatment. No significant difference was observed by the transient treatment with ZSTK474. In contrast, when cells were treated with ZSTK474 continuously (continuous treatment), the surviving fraction was lower compared to samples without the drug (Fig. 2B). The continuous treatment of cells with ZSTK474 decreased the size of colonies (Fig. 2C). The size was even smaller for colonies formed after the combined treatment using X-rays and ZSTK474 (Fig. 2C).

Effect of treatment with X-rays and/or ZSTK474 on Akt phosphorylation. Figure 3 shows *in vitro* effects of X-irradiation alone, ZSTK474 alone, or in combination on phosphorylation of Akt protein in HeLa cells. The Akt phosphorylation was almost completely inhibited by the treatment using 1 μM ZSTK474. Irradiation with 6 Gy X-rays enhanced the phosphorylation at Thr308 of Akt, although phosphorylation at Ser473 did not increase significantly. The phosphorylation of GSK-3β, a downstream molecule of Akt, was also inhibited significantly by ZSTK474 treatment. X-irradiation slightly increased the phosphorylation of GSK-3β. Treatment with ZSTK474 1 day after X-irradiation greatly decreased the phosphorylation of Akt and GSK-3β.

Effect of combined treatment against *in vivo* tumor growth in HeLa xenografts. The combined effect of X-rays and ZSTK474 against tumor growth of a HeLa xenograft model was examined. HeLa cells were inoculated on a hind leg of each mouse. When the tumor size reached approximately 150 mm^3, the tumor region was irradiated once with X-rays. One day later, treatment with ZSTK474 began, given orally. As shown in Figure 4(A), single local X-irradiation at 8 Gy alone or continuous oral administration of 100 mg/kg ZSTK474 alone inhibited the growth of s.c. implanted human HeLa tumors. X-irradiation alone or ZSTK474 alone induced only partial inhibition of tumor growth. However, the combined treatment resulted in significant total tumor growth inhibition (Fig. 4B). There were no enhancements of toxicity judged by loss of body weight in treated mice during the combined therapy (Fig. 4C). To assess toxicity, Yaguchi *et al.*[3] evaluated toxic effects for normal organs by measuring the body weight of mice and the H&E staining of femur bone marrow sections. Furthermore, chronic oral inoculation of ZSTK474 at a higher dose (800 mg/kg) over 4 weeks again reduced body weight within a tolerable range, without toxic effects to critical organs. The researchers concluded that ZSTK474 given orally to mice had strong antitumor activity against human cancer xenografts without toxic effects to critical organs.[3]

In vivo effects of X-rays and ZSTK474 on Akt signaling in tumors were examined using the IHC method. As shown in Figure 4D, ZSTK474 clearly inhibited the phosphorylation of

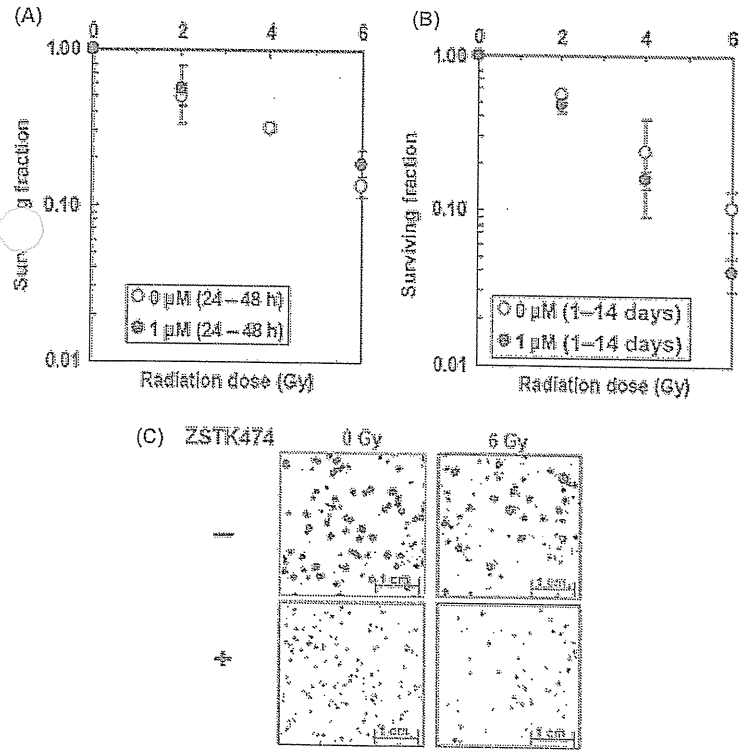

Fig. 2. (A) Clonogenic survival rate of HeLa cells treated with ZSTK474 (transient treatment; 24 h) after X-irradiation. The cells were irradiated at the indicated doses of X-ray, then 1 day later they were exposed to 1 μM ZSTK474 for 24 h. After changing the medium to ZSTK474-free medium, the cells were incubated at 37°C for 2 weeks for analysis of their colony-forming abilities. Open circles, control; closed circles, ZSTK474 treatment. Each point represents the mean survival fraction from three dishes. The graph is representative of three independent experiments. (B) Clonogenic survival rate of cells treated with ZSTK474 (continuous treatment; 14 days) after X-irradiation. The cells were irradiated at the indicated doses of X-ray, then 1 day later exposed to 1 μM ZSTK474 continuously. The cells were incubated at 37°C for 2 weeks for analysis of their colony-forming abilities. Open circles, control; closed circles, ZSTK474 treatment. Each point represents the mean survival fraction from three dishes. The graph is representative of three independent experiments. (C) Microphotographs of colonies taken 2 weeks after treatment. Upper left, control; upper right, 6 Gy X-rays only; lower left, 1 μM ZSTK474 only; lower right, combination of X-rays and ZSTK474.

doi: 10.1111/j.1349-7006.2011.01916.x

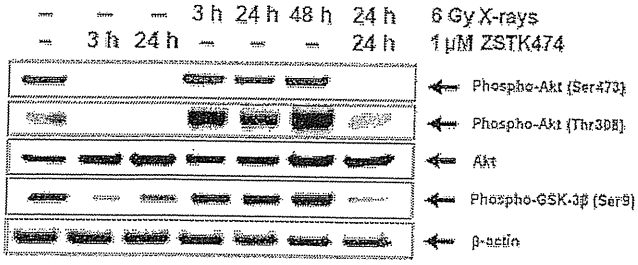

Fig. 3. Phosphorylation of Akt and GSK-3β proteins in HeLa cells treated with X-rays alone, ZSTK474 alone, or a combination of both agents. The cells were treated as indicated and analyzed by Western blotting. For the conditions without ZSTK474, DMSO was added. Lane 1 is a control (without X-irradiation or ZSTK474 treatment). The cells were harvested at 3 h or 24 h after drug exposure (lanes 2 and 3). The cells were harvested at 3, 24, or 48 h after 6 Gy X-irradiation (lanes 4, 5, and 6). The cells were irradiated with 6 Gy X-rays followed by treatment with 1 μM ZSTK474 for 24 h beginning 1 day after irradiation (lane 7).

Akt in mouse tumor on day 2. Continuous treatment with ZSTK474 after X-irradiation also inhibited the phosphorylation of Akt. Similar results were also obtained on day 15 (data not shown).

Discussion

Ionizing radiation activates the PI3K/Akt pathway,[9,10] so the PI3K survival pathway can be a major target for combined treatments. Many reports have shown the radiosensitizing effect of low molecule PI3K inhibitors *in vitro*.[11,12] However, the inhibitors extensively studied so far, such as wortmannin and LY294002, lack specificity and showed unacceptable toxicity in animal studies.[13] Recently, a new generation of PI3K inhibitors, including ZSTK474, has been developed and their *in vivo* anticancer effect has been closely examined.[3,14–18] Furthermore, their combination with other agents might be desirable for more adequate usage of the drugs in future clinical therapy. In the present study, we have clearly showed that the combination of X-rays and ZSTK474 (treated 24 h after X-rays) remarkably inhibited the proliferation of human cancer cells (HeLa) and the growth of the xenograft tumor. Only 100 mg/kg ZSTK474 was required to almost completely inhibit tumor growth *in vivo* if the tumor was X-irradiated once before treatment. A higher concentration (400 mg/kg) was required for a similar effect with ZSTK474 alone.[3]

Treatment of non-small-cell lung cancer with a combination of PI3K inhibitor and γ-irradiation *in vivo* was reported recently.[19] In the report, dual PI3K/mTOR blockade by BEZ235, a novel, orally applicable pan-PI3K inhibitor, was shown to effectively sensitize non-small-cell lung cancer to the pro-apoptotic effects of ionizing radiation both *in vivo* and *in vitro*, where BEZ235 was treated before irradiation to enhance the radiation effect. As the specificity of BEZ235 to PI3K is not high compared to ZSTK474 and considerable inhibition of DNA-PK is expected,[6] the radiosensitizing effect of BEZ235 might be partly explained by the inhibition of DNA-PK, by which the DNA repair process should be disturbed.[20] In the present study, however, we used ZSTK474, a novel, and orally applicable PI3K-specific inhibitor

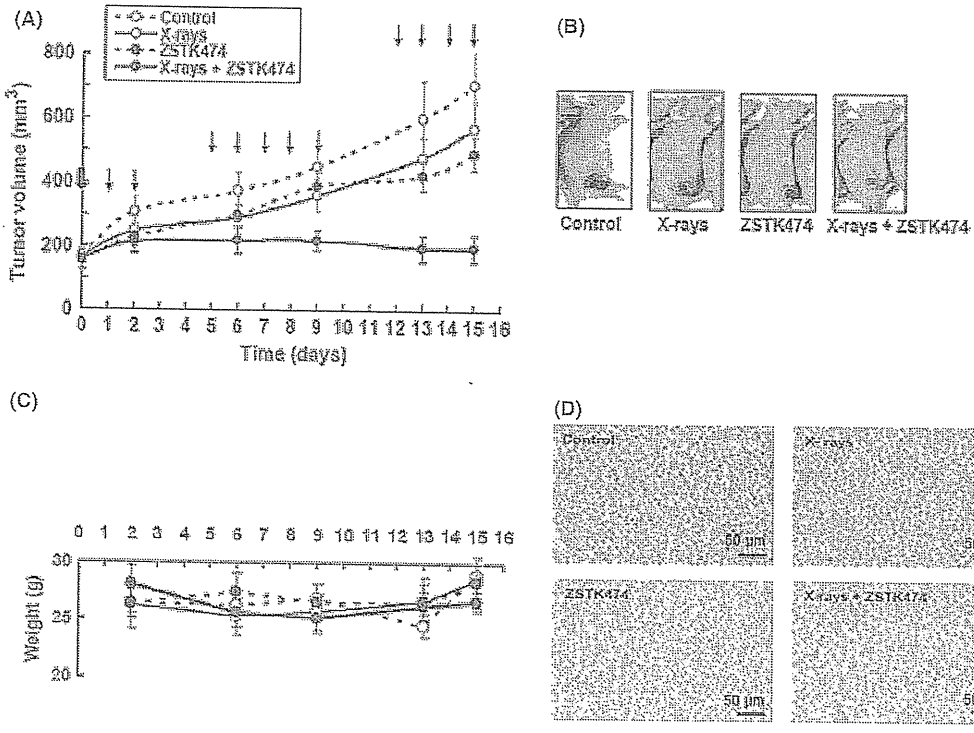

Fig. 4. (A) Xenograft growth of HeLa cells in nude mice treated as indicated. At the bold arrow (day 0), the tumors were irradiated with 8 Gy X-rays (groups 2 and 4). Beginning 1 day after X-irradiation (day 1), ZSTK474 (100 mg/kg) was given orally every day (groups 3 and 4) until day 15 except for days 3, 4, 10, and 11. We irradiated the tumor on day 0, then started the first drug dosage on days 1 and 2. The following week, we gave the agent everyday from day 5 to day 9. In the third week, we gave the agent every day from day 12 to day 15. Mice were killed on day 15. Subsequently, those tumor tissues were extracted for immunohistochemical analysis. Points are mean of tumor volume (mm^3) of each treatment ($n = 6$). Bars show SD. (B) Weight change of the mice during the time course shown. (C) Photographs of mice on day 15, showing those with tumor size close to the average for each group. The mice were anesthetized. (D) Effect of treatment with X-rays alone, ZSTK474 alone, or in combination on phosphorylation of Akt measured by immunohistochemical analysis of HeLa xenografts on day 2. Upper left, control; upper right, 8 Gy X-rays; lower left, ZSTK474 100 mg/kg; lower right, X-rays + ZSTK474.

after X-ray treatment. The timing of ZSTK474 application was 24 h after irradiation, so the DNA repair process related to DNA-PK should be completed.[20] Therefore, inhibition of DNA-PK by ZSTK474, even if such activity is present, is not likely to be the major mechanism for the significant combination effect observed in the present study.

A strong combination effect was observed for *in vitro* cell proliferation assay when the cells were treated for a longer time with ZSTK474. The colony-forming assay also showed that continuous treatment, rather than transient treatment (24 h), significantly reduced the surviving fraction after X-irradiation. This reduction in the surviving fraction might be due to the strong inhibition of cell proliferation by ZSTK474, especially after treatment with X-rays, rather than the induction of actual cell death. This interpretation is supported by colony sizes, where ZSTK474 treatment alone remarkably reduced the colony sizes, but the effect was stronger for cells irradiated first then treated with the drug. ZSTK474 alone does not induce apoptosis.[3,5] A significant difference in the number of apoptotic cells was not observed in the tumor between the samples treated with X-rays alone and with the combination of X-rays and ZSTK474 (data not shown).

ZSTK474 alone significantly inhibited phosphorylation of Akt and its downstream molecule GSK-3β. In contrast, X-irradiation enhanced the phosphorylation of Akt and GSK-3β. The activation of PI3K/Akt signaling is associated with the radioresistance of many cancer cells.[21–23] When ZSTK474 was applied after X-irradiation, the enhancement of the activation of Akt and GSK-3β was reversed and the reduced phosphorylation of these proteins was observed. It is postulated that the activation of the PI3K pathway in irradiated tumors is an important survival strategy for these cells. However, to understand the molecular mechanism(s) of the therapeutic efficacy of this combination, its effects on other survival or death factors should be examined. Therefore, treatment with ZSTK474 after X-irradiation leading to the inhibition of PI3K pathway, which the irradiated cells try to activate, might be related to effective tumor growth inhibition, observed by the combination treatment in this study.

In this study, we clearly showed that the combination of ZSTK474 with X-rays (continuous application of ZSTK474 after X-irradiation) results in dramatic tumor growth inhibition *in vitro* and *in vivo*. Although the precise molecular mechanism to explain these results remains to be elucidated, this phenomenon might be worth exploring for clinical application. An alternative sequence, X-irradiation after ZSTK474, should be examined next. Furthermore, combination with heavy-ion radiotherapy, an effective cancer therapy modality for certain tumors, is also a fascinating theme.

Acknowledgments

This work was partly supported by: grants from the National Institute of Biomedical Innovation of Japan (5-13); Grants-in-Aid for the Priority Area "Cancer" and "New Research Categories" from the Ministry of Education, Culture, Sports, Science, and Technology of Japan (20200039, 18015049, 20015048); Grants-in-Aid for Scientific Research from the Japan Society for the Promotion of Science (17390032 and 20790087); and a grant from the Kobayashi Institute for Innovative Cancer Chemotherapy. We thank Ms. Mitsuko Takusagawa of NIRS for her help with cell culture and clonogenic survival assays.

Disclosure Statement

T. Yamori and R. Okayasu were partly supported by a research grant from Zenyaku Kogyo Co. H. Yoshimi, S. Yaguchi and J. Enami are employee of Zenyaku Kogyo Co.

References

1 Kong D, Okamura M, Yoshimi H, Yamori T. Antiangiogenic effect of ZSTK474, a novel phosphatidylinositol 3-kinase inhibitor. *Eur J Cancer* 2009; 45: 857–65.
2 Kong D, Yamori T. Advances in development of phosphatidylinositol 3-kinase inhibitors. *Curr Med Chem* 2009; 16: 2839–54.
3 Yaguchi S, Fukui Y, Koshimizu I *et al.* Antitumor activity of ZSTK474, a new phosphatidylinositol 3-kinase inhibitor. *J Natl Cancer Inst* 2006; 98: 545–56.
4 Kong D, Yamori T. ZSTK474 is an ATP-competitive inhibitor of class I phosphatidylinositol 3 kinase isoforms. *Cancer Sci* 2007; 98: 1638–42.
5 Dan S, Yoshimi H, Okamura M, Mukai Y, Yamori T. Inhibition of PI3K by ZSTK474 suppressed tumor growth not via apoptosis but G0/G1 arrest. *Biochem Biophys Res Commun* 2009; 379: 104–9.
6 Kong D, Yaguchi S, Yamori T. Effect of ZSTK474, a novel phosphatidylinositol 3-kinase inhibitor, on DNA-dependent protein kinase. *Biol Pharm Bull* 2009; 32: 297–300.
7 Hall EJ, Giaccia AJ. *Radiobiology for the Radiologist*. Philadelphia: Lippincott Williams & Wilkins, 2006.
8 Yamori T, Iizuka Y, Takayama Y *et al.* Insulin-like growth factor I rapidly induces tyrosine phosphorylation of a Mr 150 000 and a Mr 160 000 protein in highly metastatic mouse colon carcinoma 26 NL-17 cells. *Cancer Res* 1991; 51: 5859–65.
9 Sunavala-Dossabhoy G, Fowler M, De Benedetti A. Translation of the radioresistance kinase TLK1B is induced by gamma-irradiation through activation of mTOR and phosphorylation of 4E-BP1. *BMC Mol Biol* 2004; 5: 1.
10 Reits EA, Hodge JW, Herberts CA *et al.* Radiation modulates the peptide repertoire, enhances MHC class I expression, and induces successful antitumor immunotherapy. *J Exp Med* 2006; 203: 1259–71.
11 Kubota N, Ozawa F, Okada S, Inada T, Komatsu K, Okayasu R. The phosphatidylinositol 3-kinase inhibitor wortmannin sensitizes quiescent but not proliferating MG-63 human osteosarcoma cells to radiation. *Cancer Lett* 1998; 133: 161–7.
12 Hosoi Y, Miyachi H, Matsumoto Y *et al.* A phosphatidylinositol 3-kinase inhibitor wortmannin induces radioresistant DNA synthesis and sensitizes cells to bleomycin and ionizing radiation. *Int J Cancer* 1998; 78: 642–7.
13 Gupta AK, Cerniglia GJ, Mick R *et al.* Radiation sensitization of human cancer cells in vivo by inhibiting the activity of PI3K using LY294002. *Int J Radiat Oncol Biol Phys* 2003; 56: 846–53.
14 Garlich JR, De P, Dey N *et al.* A vascular targeted pan phosphoinositide 3-kinase inhibitor prodrug, SF1126, with antitumor and antiangiogenic activity. *Cancer Res* 2008; 68: 206–15.
15 Maira SM, Stauffer F, Brueggen J *et al.* Identification and characterization of NVP-BEZ235, a new orally available dual phosphatidylinositol 3-kinase/mammalian target of rapamycin inhibitor with potent in vivo antitumor activity. *Mol Cancer Ther* 2008; 7: 1851–63.
16 Folkes AJ, Ahmadi K, Alderton WK *et al.* The identification of 2-(1H-indazol-4-yl)-6-(4-methanesulfonyl-piperazin-1-ylmethyl)-4-morpholin -4-yl-thieno[3,2-d]pyrimidine (GDC-0941) as a potent, selective, orally bioavailable inhibitor of class I PI3 kinase for the treatment of cancer. *J Med Chem* 2008; 51: 5522–32.
17 Fan QW, Cheng CK, Nicolaides TP *et al.* A dual phosphoinositide-3-kinase alpha/mTOR inhibitor cooperates with blockade of epidermal growth factor receptor in PTEN-mutant glioma. *Cancer Res* 2007; 67: 7960–5.
18 Ihle NT, Williams R, Chow S *et al.* Molecular pharmacology and antitumor activity of PX-866, a novel inhibitor of phosphoinositide-3-kinase signaling. *Mol Cancer Ther* 2004; 3: 763–72.
19 Konstantinidou G, Bey EA, Rabellino A *et al.* Dual phosphoinositide 3-kinase/mammalian target of rapamycin blockade is an effective radiosensitizing strategy for the treatment of non-small cell lung cancer harboring K-RAS mutations. *Cancer Res* 2009; 69: 7644–52.
20 Okayasu R, Suetomi K, Ullrich RL. Wortmannin inhibits repair of DNA double-strand breaks in irradiated normal human cells. *Radiat Res* 1998; 149: 440–5.
21 Tanno S, Yanagawa N, Habiro A *et al.* Serine/threonine kinase AKT is frequently activated in human bile duct cancer and is associated with increased radioresistance. *Cancer Res* 2004; 64: 3486–90.
22 Tomioka A, Tanaka M, De Velasco MA *et al.* Delivery of PTEN via a novel gene microcapsule sensitizes prostate cancer cells to irradiation. *Mol Cancer Ther* 2008; 7: 1864–70.
23 Li HF, Kim JS, Waldman T. Radiation-induced Akt activation modulates radioresistance in human glioblastoma cells. *Radiat Oncol* 2009; 4: 43.

doi: 10.1111/j.1349-7006.2011.01916.x

pubs.acs.org/acschemicalbiology

Identification of SAP155 as the Target of GEX1A (Herboxidiene), an Antitumor Natural Product

Makoto Hasegawa,[†] Tatsuhiro Miura,[†] Kouji Kuzuya,[†] Ayu Inoue,[†] Se Won Ki,[‡] Sueharu Horinouchi,[‡] Tetsuo Yoshida,[§] Tatsuki Kunoh,[†] Koichi Koseki,[†] Koshiki Mino,[†] Ryuzo Sasaki,[†] Minoru Yoshida,[∥] and Tamio Mizukami[†,*]

[†]Nagahama Institute of Bio-Science and Technology, Nagahama, Shiga 526-0829, Japan

[‡]Department of Biotechnology, The University of Tokyo, Bunkyo-ku, Tokyo 113-8657, Japan

[§]Innovative Drug Research Laboratories, Kyowa Hakko Kirin Co. Ltd., Machida, Tokyo 194-8533, Japan

[∥]Chemical Genetics Laboratory, RIKEN, Wako, Saitama 351-0198, Japan

Supporting Information

ABSTRACT: GEX1A is a microbial product with antitumor activity. HeLa cells cultured with GEX1A accumulated $p27^{Kip}$ and its C-terminally truncated form p27*. GEX1A inhibited the pre-mRNA splicing of p27, producing p27* from the unspliced mRNA containing the first intron. p27* lacked the site required for E3 ligase-mediated proteolysis of p27, leading to its accumulation in GEX1A-treated cells. The accumulated p27* was able to bind to and inhibit the cyclin E-Cdk2 complex that causes E3 ligase-mediated degradation of p27, which probably triggers the accumulation of p27. By using a series of photoaffinity-labeling derivatives of GEX1A, we found that GEX1A targeted SAP155 protein, a subunit of SF3b responsible for pre-mRNA splicing. The linker length between the GEX1A pharmacophore and the photoreactive group was critical for detection of the GEX1A-binding protein. GEX1A serves as a novel splicing inhibitor that specifically impairs the SF3b function by binding to SAP155.

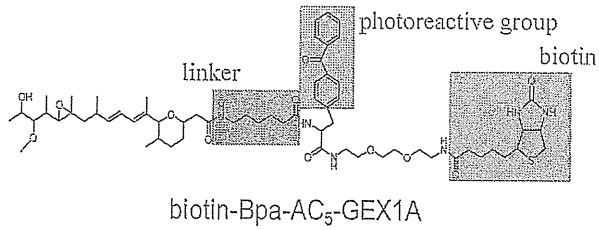

biotin-Bpa-AC_5-GEX1A

GEX1A (see Supplementary Figure S4) was isolated as a natural substance with *in vivo* antitumor activity from a culture broth of *Streptomyces* sp.[1] This compound causes cell cycle arrest in G1 and G2/M phases in the normal human fibroblast cell line WI-38.[2] These effects were confirmed in HeLa cells (Supplementary Figure S1), which were used throughout the experiments in this study.

The cell cycle in mammalian cells is driven by the periodic activation of cyclin-dependent kinases (Cdks). Activation of Cdks requires binding of the catalytic subunits Cdk4/6, Cdk2, and Cdk1 with their specific regulatory subunits known as cyclins D, E, A, and B. These kinase activities are further regulated in complex manners including cyclin-kinase inhibitors (CdkIs).[3] Since $p27^{Kip}$ (Cdk inhibitory protein, hereafter referred to as p27) is a key component of CdkIs of the G1 transition,[3] we examined the effects of GEX1A on the level of p27. Treatment of HeLa cells with GEX1A caused p27 accumulation in time- and dose-dependent manners (Figure 1, panels A, B). In addition to full-size p27 (27 kDa), a band with a smaller size (22 kDa, referred to as p27*) increased after the drug treatment. These two bands were both detected with an antibody against full-size p27 (amino acids 1−198). An antibody against the C-terminal peptide of p27 (amino acids 181−198) detected full-size p27 but not p27* (Figure 1, panel C), suggesting that p27* was a truncated form of p27 that lacked the C-terminal portion. It has been reported that cells treated with spliceostatin A, a newly identified splicing inhibitor, produce a C-terminally truncated form of p27.[4] Therefore, we examined whether GEX1A inhibited the pre-mRNA splicing of p27, producing p27*. Figure 2 (panel A) depicts the exon-intron disposition of the primary transcript of the *p27* gene. It also shows the mature mRNA (species 1) and unspliced RNA species (species 2−4) as well as their predicted RT-PCR products. Notably the first intron contained an in-frame translational termination codon. If RNA species containing intron 1 (species 3 and 4) are exported to the cytoplasm and somehow overcome the nonsense-mediated mRNA decay (NMD),[5] these RNAs could give rise to p27* consisting of the C-terminally truncated p27 (158 amino acids) and the peptide encoded by the intronic sequence (21 amino acids). The production of p27* in GEX1A-treated cells suggested that the drug perturbed the mRNA splicing. Therefore, we performed RT-PCR to examine whether treatment of cells with GEX1A led to the production of unspliced RNAs of p27. All of the predicted unspliced species were detected in cells cultured with GEX1A, while these species were almost undetectable in untreated cells and only the mature mRNA was found

Received: August 17, 2010
Accepted: December 2, 2010
Published: December 07, 2010

dx.doi.org/10.1021/cb100248e | *ACS Chem. Biol.* 2011, 6, 229–233

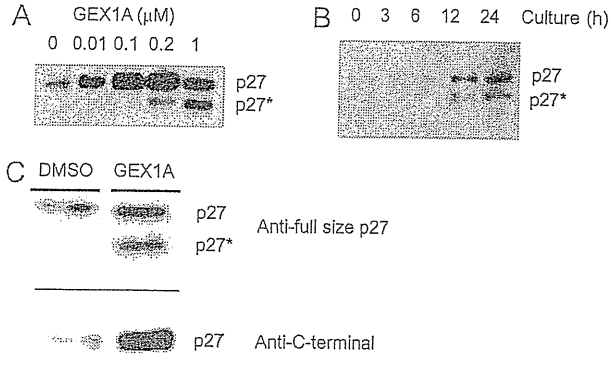

Figure 1. GEX1A causes accumulation of p27 and its C-terminally truncated form p27*. Both proteins were detected by Western blotting. (A) HeLa cells were incubated with the indicated concentrations of GEX1A for 24 h. p27 and p27* in the cell lysates were detected using an antibody against full-size p27. (B) HeLa cells were incubated with 0.2 μM GEX1A for the indicated periods. p27 and p27* in the lysates were detected using the antibody against full-size p27. (C) HeLa cells were incubated for 24 h with 1 μM GEX1A or with DMSO alone as a control. p27 and p27* in the lysates were detected using the antibody against full-size p27 (top) or an antibody against the C-terminal peptide of p27 (bottom).

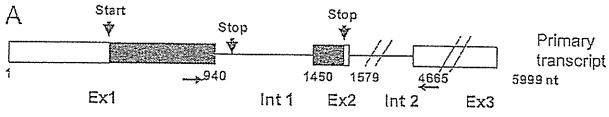

Predicted products (bp)	Possible RNA species
583	1: Ex1-Ex2-Ex3
2669	2: Ex1-Ex2-Int2-Ex3,
1093	3: Ex1-Int1-Ex2-Ex3
3179	4: Ex1-Int1-Ex2-Int2-Ex3

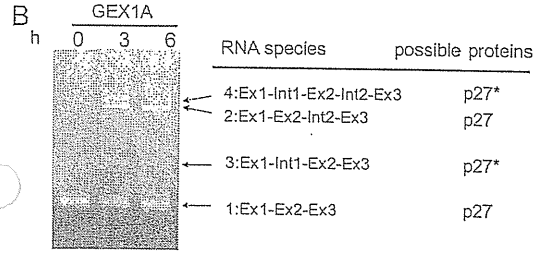

Figure 2. GEX1A inhibits the pre-mRNA splicing of p27. (A) Exon (Ex)-intron (Int) disposition of the p27 primary transcript and possible RNA species produced when splicing of the pre-mRNA is inhibited. The white rectangles indicate noncoding regions, and the black rectangles indicate coding regions. The sites for the start and stop of translation are shown. The horizontal arrows indicate the primer positions used for RT-PCR. The predicted RT-PCR products (bp) and the corresponding RNA species are also shown. (B) HeLa cells were incubated with 1 μM GEX1A for the indicated periods, and the p27-related RNA species were detected by RT-PCR. The middle column shows the RNA species. Possible proteins produced by these RNA species are shown in the right column.

(Figure 2, panel B). We confirmed that GEX1A is an inhibitor of universal pre-mRNA splicing by analyzing the transcripts of other three genes (*DNAJB1*, *BRD2*, and *RIOK3*). The unspliced RNA species of these genes were produced in dose-dependent manners (Supplementary Figure S2).

Once mRNAs have been exported to the cytoplasm, they are subjected to quality control in the pioneering round of translation. NMD is one of the surveillance pathways that direct the degradation of translationally abnormal mRNAs.[5] NMD eliminates mRNAs containing a premature termination codon (PTC) for translation. The exon−exon junction complex (EJC) plays an important role in NMD. An EJC is deposited at −20 to −40 nucleotides upstream of an exon−exon junction.[6,7] In the normal mRNA, all of the EJCs are removed in the pioneering round of translation, which qualifies polyribosome formation for subsequent rounds of translation. When a PTC is present upstream of an EJC, a ribosome pauses at the PTC and does not reach the EJC to be removed. As a rule, the location of a PTC at >50−55 nucleotides upstream of an exon−exon junction has been thought to leave an EJC on mRNAs, which is a signal that elicits NMD.[8] In this context, the EJCs on the unspliced RNA species 2 of p27 (Ex1-Ex2-Int2-Ex3) as well as those on the mature mRNA (species 1) can be removed and species 2 may therefore contribute to p27 production in addition to the mature mRNA. Species 4 (Ex1-Int1-Ex2-Int2-Ex3) does not bind to an EJC and probably escapes NMD, producing p27*. However, species 3 (Ex1-Int1-Ex2-Ex3) may retain an EJC on exon 2 after the pioneering round of translation, leading to NMD-mediated degradation.

Next we discuss possible mechanisms of accumulation of p27* and p27. The level of p27 varies during the cell cycle. It is reduced in G1 and S phases so that the cell cycle can progress through these two phases.[9] The concentration of p27 is predominantly regulated by the ubiquitin-proteasome pathway.[10] Degradation of p27 through this pathway is triggered by the phosphorylation of Thr187 by cyclin E-Cdk2.[11] Since p27* lacks Thr187, it is capable of escaping from E3 ligase-mediated proteolysis, resulting in the accumulation of p27* in GEX1A-treated cells. How does GEX1A lead to the accumulation of p27? GEX1A did not increase p27 mRNA (see Figure 2, panel B). It is likely that the inhibition of cyclin E-Cdk2 by p27* (see below) triggers the accumulation of p27. The accumulation of p27 and p27* is probably exceptional, since the levels of most proteins would be decreased when splicing of their primary transcripts are inhibited.

p27 binds to the cyclin E or A-Cdk2 complex and inhibits its activity.[3] We therefore examined whether p27* was still able to bind to the Cdk2 complex. The Cdk2-associated p27 increased after treatment with GEX1A, and notably, p27* increased (Supplementary Figure S3, panel A). The Cdk2 activity in the immunoprecipitates obtained with either the anti-Cdk2 antibody or the anticyclin E antibody markedly decreased upon treatment with GEX1A (Supplementary Figure S3, panel B). Conceivably, p27* is functionally active and inactivates cyclin E-Cdk2, because the sites in p27 required for binding with the cyclin-Cdk complex are located in the N-terminal region,[12] which remains in p27*.

The excision of introns from pre-mRNAs is carried out by a multiprotein-RNA complex known as the spliceosome.[13,14] The core spliceosome consists of five small nuclear RNAs (snRNAs U1, U2, U4, U5, and U6) and associated proteins, forming snRNA-protein complexes (snRNPs). U2 snRNP consists of U2 snRNA, splicing factors SF3a and SF3b, and other proteins. The SF3b complex consists of seven spliceosome-associated proteins (SAPs), namely, SAP155, SAP145, SAP130, SAP49, SAP14a, SAP14b, and SAP10.[15] We designed three GEX1A derivatives as

dx.doi.org/10.1021/cb100248e |ACS Chem. Biol. 2011, 6, 229–233

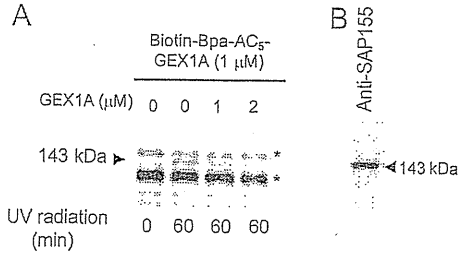

Figure 3. Photoaffinity labeling of the 143-kDa protein is inhibited by GEX1A. (A) Nuclear extracts from HeLa cells were incubated with 1 μM biotin-Bpa-AC$_5$-GEX1A in the absence or presence (1 or 2 μM) of GEX1A for 16 h. The samples were exposed to UV light (365 nm, 6 W) for 60 min. After SDS−PAGE, the proteins were electroblotted onto a membrane, and the photoaffinity-labeled proteins were detected by chemical luminescence using HRP-conjugated streptoavidin. The asterisks indicate nonspecific bands. (B) The same membrane was used for the detection of SAP155 with its antibody.

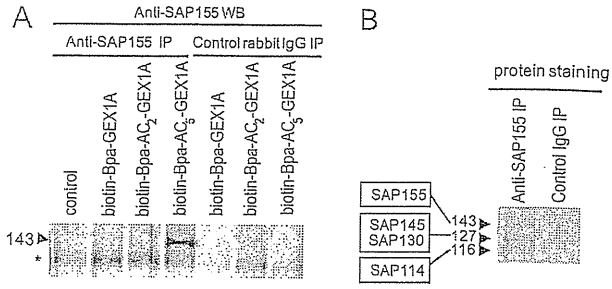

Figure 4. The photoaffinity-labeled protein of 143 kDa is SAP155. (A) Nuclear extracts from HeLa cells were incubated with 1 μM GEX1A derivatives for 16 h. The samples were exposed to UV light for 60 min and immunoprecipitated with an anti-SAP155 antibody or a control IgG. The proteins in the immunoprecipitates were separated by SDS−PAGE and electroblotted onto a membrane, and the photoaffinity-labeled proteins were detected as in Figure 3. The asterisk indicates a nonspecific band. (B) Nuclear extracts from HeLa cells were immunoprecipitated with the anti-SAP155 antibody or control IgG. Proteins in the immunoprecipitates were separated by SDS−PAGE and visualized by silver staining. Three protein bands of 143, 127, and 116 kDa were analyzed by in-gel digestion and subsequent LC−MS/MS. These bands were identified as SAP155, SAP145 + SAP130, and SAP114, respectively (see Supplementary Table S11).

probes to identify the spliceosome proteins interacting with GEX1A (Supplementary Figure S4). A photoreactive amino acid (*p*-benzoylphenylalanine, Bpa) was introduced into GEX1A at the carboxylic acid with linkers of various lengths between this amino acid and GEX1A. The photoreactive amino acid was converted to a triplet state by UV light and thereby covalently bound to C−H bonds in the binding protein. A biotin moiety was also included for detection of the labeled protein with HRP-conjugated streptavidin. The GEX1A derivatives were confirmed to be the expected compounds by mass spectrometry (MS) (Supplementary Figure S5). All of the derivatives showed inhibition of splicing but with different potencies (Supplementary Figure S6). These different potencies may be derived from differences in the membrane permeability, intracellular stability and affinity for the target protein.

To identify the spliceosome proteins that bound to the GEX1A derivatives, nuclear extracts of HeLa cells treated with the derivatives were subjected to the photocross-linking reaction. After the separated nuclear proteins were electroblotted onto a membrane, the labeled proteins were detected. Among the three photoreactive GEX1A derivatives, only biotin-Bpa-AC$_5$-GEX1A yielded a labeled protein band of 143 kDa (Supplementary Figure S7). The formation of this 143-kDa protein band was almost completely inhibited by the presence of a 2-fold excess of GEX1A (Figure 3, panel A). When the same membrane was subjected to immunoblotting, the 143-kDa band corresponded to SAP155, a subunit in the SF3b complex (Figure 3, panel B).

To confirm that the photoaffinity-labeled 143-kDa band was SAP155, the nuclear extracts after treatment with the GEX1A derivatives were immunoprecipitated with an anti-SAP155 antibody. After the precipitated proteins were separated and electroblotted onto a membrane, the labeled proteins were detected. A clear band of 143 kDa was observed only when biotin-Bpa-AC$_5$-GEX1A was used for the labeling (Figure 4, panel A), consistent with the notion that this ligand is able to bind to the 143-kDa protein. The proteins immunoprecipitated from the nuclear extracts using the anti-SAP155 antibody were separated and visualized by protein staining. Three bands of 116, 127, and 143 kDa were observed (Figure 4, panel B). These protein bands were identified by in-gel trypsin digestion and subsequent LC−MS/MS analysis. The MASCOT program matched the 143-kDa MS/MS ion sequences to SAP155 (Supplementary Table S1). These results indicate that GEX1A inhibits splicing of the pre-mRNA through binding with SAP155.

Although all derivatives showed inhibitory effects on pre-mRNA splicing (Supplementary Figure S6), only biotin-Bpa-AC$_5$-GEX1A was able to label SAP155, a subunit of the SF3b complex. A close proximity of the photoreactive group to the surface of the SF3b subunit may be necessary for efficient cross-linking. The length of the linker between the Bpa residue and GEX1A appeared to be critical for the cross-linking, and biotin-Bpa-AC$_5$-GEX1A had the longest linker of 7 Å.

The primary transcripts of most eukaryotic genes are retained in the nucleus until their introns are removed by the spliceosome. GEX1A inhibited pre-mRNA splicing, producing unspliced RNA species of the *p27* gene. At least one of the unspliced RNAs containing the first intron is exported to the cytoplasm where it is translated to produce p27*. Furthermore, GEX1A exerts its inhibitory effect on the splicing through binding with SAP155, a subunit of SF3b. Presumably GEX1A-derived inactivation of SF3b makes it possible for unspliced pre-mRNAs to emerge into the cytoplasm. These results support a previous proposal [4] that SF3b has a dual function in pre-mRNA processing, namely the removal of introns and the nuclear retention of unspliced RNAs.

Recently, two natural products were reported to inhibit pre-mRNA splicing. Spliceostatin A may interact with SAP130 or SAP155,[4] and pladienolide B binds to SAP130.[16] Regarding their structures, spliceostatin A is considerably different from GEX1A, while pladienolide B is similar to GEX1A except that GEX1A lacks a macrolide ring (Supplementary Figure S8). A photoreactive derivative of pladienolide B was cross-linked to SAP130 but not SAP155. These distinct results between GEX1A and pladienolide B imply that an interface between SAP155 and SAP130 in the SF3b complex is located near the binding sites for these inhibitors. Detailed mapping of the GEX1A-binding site is underway. Crucial roles of SAP155 in the splicing machinery have been amply documented.[17,18] Moreover, the functions of SAP155 are regulated by its phosphorylation-dephosphorylation balance.[19] Thus elucidation of the GEX1A-binding site in

dx.doi.org/10.1021/cb100248e |ACS Chem. Biol. 2011, 6, 229–233

SAP155 is important for better understanding of not only the inhibitory mechanism but also the regulation of SAP155. Chemical-derived inactivation of SF3b appears to disrupt the cellular function required for nuclear retention of unspliced pre-mRNAs (ref 4 and this paper). Such chemicals would be very useful for elucidating the molecular mechanism that links the inhibition of splicing and the leakage of unspliced pre-mRNAs. All of the three compounds have antitumor activity, indicating that the splicing machinery is a novel target for antitumor drugs and that further modification of these chemicals may lead to the development of drugs with high efficacy.

METHODS

GEX1A, Cells, and Western Blotting. GEX1A was supplied by Kyowa Hakko Kirin Co. Ltd. and was dissolved in DMSO. The final concentration of DMSO was adjusted to 0.1%. Controls contained 0.1% DMSO alone. HeLa cells were cultured in RPMI medium containing 10% FBS, 100 units/mL penicillin and 0.1 mg/mL streptomycin. The cells were incubated in NP40 lysis buffer consisting of 50 mM HEPES pH 7.4, 250 mM NaCl, 1% NP-40, 5 mM β-glycerophosphate, 2 mM Na_3VO_4, 0.2 mM EDTA, 10 mM NaF, 1 mM DTT, 1% Halt Protease Inhibitor Cocktail (Pierce), and 1 mM PMSF. The lysates were centrifuged and the protein concentrations of the supernatants were determined by the Quick Start Protein Assay (Bio-Rad). The proteins were analyzed by Western blotting with the following primary antibodies against human proteins purchased from Santa Cruz Biotechnology: antifull-size p27 (amino acids 1−198) (1:200), anti-C-terminal peptide of p27 (amino acids 181−198) (1:100), and anti-β-actin (1:1000). As secondary antibodies, HRP-conjugated antimouse IgG (1:5000; Calbiochem) and HRP-conjugated anti-rabbit IgG (1:5000; Invitrogen) were used. When the antibody against the C-terminal peptide of p27 was used, a solution for signal enhancement (Can Get Signal Immunoprecipitation Solution; Toyobo) was used according to the manufacturer's protocol.

RT-PCR. Total RNA was extracted using an RNeasy Mini Kit (Qiagen). RT-PCR was conducted with ReverTra Ace-α (Toyobo) using 0.3 μg of RNA. The primers used for p27 were 5′-GCAAGTA-CGAGTGGCAAGAGG-3′ for exon 1 and 5′-TCCAACGCTTTTA-GAGGCAGA-3 for exon 3.

Chemical Synthesis. Photoaffinity-labeling GEX1A derivatives were synthesized using linker moieties (β-alanine or 6-aminohexanoic acid), *p*-benzoylpehenylalanine (Bpa), and biotin-PEO-amine (EZ-Link Biotin Reagents; Thermo Fisher Scientific). In each step, the carboxyl group in a GEX1A derivative was esterified with 3 equiv of *N*-hydroxysuccinimide (HOSu) by treatment with 3 equiv of water-soluble carbodiimide in dimethylformamide (DMF) containing 3 equiv of triethylamine (TEA). A GEX1A-HOSu derivative was mixed with an amine component (3−4 equiv of a linker moiety) in a DMF/water mixed solvent containing 3 equiv of TEA. After reaction for 4−22 h at 30 °C, each product was purified using a Cosmosil AR-II 5C18 column (Nacalai Tesque) and an HPLC (Gilson). The HPLC was carried out at a flow rate of 1 mL/min with a linear gradient of 10−50% CH_3CN in 10 mM sodium acetate (pH 5.7). The eluates from the HPLC column were monitored at 220 nm, and their contents were analyzed by ESI IT-TOF mass spectrometry (LCMS-IT-TOF System; Shimadzu).

Nuclear Extract Preparation. Cold PBS-washed HeLa cells (1×10^9 cells) were suspended in two volumes of buffer A (10 mM Tris-HCl pH 7.9, 10 mM KCl, 1.5 mM $MgCl_2$, 0.5 mM DTT, 0.5 mM PMSF) and homogenized by 30 strokes of a glass Dounce homogenizer. After centrifugation of the homogenate, the precipitate was squeezed by 10 strokes of the glass homogenizer in 2.5 mL of buffer A containing 420 mM NaCl. After 30 min of stirring, the insoluble matter was removed by centrifugation. The supernatant was dialyzed against buffer B (20 mM Tris-HCl pH 7.9, 100 mM KCl, 0.2 mM EDTA, 0.5 mM DTT, 0.5 mM PMSF, 20% glycerol). Aliquots were stored at −80 °C until analysis.

Immunoprecipitation. An anti-SAP155 antibody (2 μg; Bethyl Laboratories) was added to a nuclear extract and mixed gently on a rotator. Protein G-agarose was added and mixed. The agarose beads were precipitated and washed with 50 mM Tris-HCl (pH 7.5) containing 150 mM NaCl and 0.05% Tween-20). Coprecipitated proteins were eluted into the SDS−PAGE sample buffer by boiling the beads for 5 min.

Protein Identification by MS. Protein bands in SDS−PAGE gels visualized by staining with a Silver Stain MS Kit (Wako Pure Chemical Industries) were excised and rinsed with 50 mM $NaHCO_3$/50% acetonitrile. The gel particles were dried in a vacuum concentrator and rehydrated in 50 μL of 50 mM $NaHCO_3$ buffer containing 10 ng/μL sequencing grade trypsin (Sigma-Aldrich). After removing the excess trypsin solution, the gel particles were overlaid with 30 μL of 50 mM $NaHCO_3$ and incubated for 16 h at 37 °C to extract trypsin-digested peptides. The supernatants containing the peptides were subsequently used for MS analysis. Each sample was loaded onto a nano-LC equipped with a PicoFrit column (New Objective). A Prominence Nano binary pump system (Shimadzu) was programmed to elute the peptides with a gradual ramp of a linear gradient of 5−90% acetonitrile with 0.1% formic acid over 60 min. The flow rate in the column was 200 nL/min, and the column end was directly connected to the nanospray tip of an LCMS-IT-TOF System (Shimadzu). The mass spectrometer was set to a cycle of one full mass scan, followed by three tandem mass scans of the three most intense ions. All the tandem mass spectra obtained were searched for in the Swiss-Prot database using the MASCOT program (Matrix Science).

ASSOCIATED CONTENT

Supporting Information. This material is available free of charge *via* the Internet at http://pubs.acs.org.

AUTHOR INFORMATION

Corresponding Author
*Phone: +81-749-64-8169. Fax: +81-749-64-8140. E-mail: mizukami@nagahama-i-bio.ac.jp.

ACKNOWLEDGMENT

We thank S. Ikeda, Y. Mukai, and A. Yamamoto for helpful discussions. This research was supported in part by Grants-in-Aid to M.H. from the Japanese Ministry of Education, Culture, Sports, Science and Technology.

REFERENCES

(1) Sakai, Y., Yoshida, T., Ochiai, K., Uosaki, Y., Saitoh, Y., Tanaka, F., Akiyama, T., Akinaga, S., and Mizukami, T. (2002) GEX1 compounds, novel antitumor antibiotics related to herboxidiene, produced by *Streptomyces* sp. I. Taxonomy, production, isolation, physicochemical properties and biological activities. *J. Antibiot. 55*, 855–862.

(2) Sakai, Y., Tsujita, T., Akiyama, T., Yoshida, T., Mizukami, T., Akinaga, S., Horinouchi, S., Yoshida, M., and Yoshida, T. (2002) GEX1 compounds, novel antitumor antibiotics related to herboxidiene, produced by *Streptomyces* sp. II. The effects on cell cycle progression and gene expression. *J. Antibiot. 55*, 863–872.

(3) Abde, M., Abukhdeir, A. M., and Park, B. H. (2008) p21 and p27: roles in carcinogenesis and drug resistance. *Expert Rev. Mol. Med. 10*, e19.

(4) Kaida, D., Motoyoshi, H., Tashiro, E., Nojima, T., Hagiwara, M., Ishigami, K., Watanabe, H., Kitahara, T., Yoshida, T., Nakajima, H., Tani,

dx.doi.org/10.1021/cb100248e |*ACS Chem. Biol.* 2011, 6, 229–233

T., Horinouchi, S., and Yoshida, M. (2007) Spliceostatin A targets SF3b and inhibits both splicing and nuclear retention of pre-mRNA. *Nat. Chem. Biol. 3,* 576–583.

(5) Isken, O., and Maquat, L. E. (2007) Quality control of eukaryotic mRNA: safeguarding cells from abnormal function. *Genes Dev. 21,* 1833–1856.

(6) Le Hir, H., Izaurralde, E., Maquat, L. E., and Moore, M. J. (2000) The spliceosome deposits multiple proteins 20−24 nucleotides upstream of mRNA exon-exon junctions. *EMBO J. 19,* 6860–6869.

(7) Le Hir, H., Gartfield, D., Izaurralde, E.., and Morre, M. J. (2001) The exon-exon junction complex provides a binding platform for factors involved in mRNA export and nonsense-mediated mRNA decay. *EMBO J. 20,* 4987–4997.

(8) Nagy, E., and Maquat, L. E. (1998) A rule for termination-codon position within intron-containing genes: When nonsense affects RNA abundance. *Trends Biochem. Soc. 23,* 198–199.

(9) Malek, N. P., Sundberg, H., McGrew, S., Nakayama, K., Kyriakidis, T. R., and Roberts, J. M. (2001) A mouse knock-in model exposes sequential proteolytic pathways that regulates $p27^{Kip1}$ in G1 and S phase. *Nature 413,* 323–327.

(10) Pagano, M., Tam, S. W., Theodoras, A. M., Beer-Romero, P., Del Sal, G., Chan, V., Yew, P. R., Draetta, G. F., and Rolfe, M. (1995) Role of the ubiquitin-proteasome pathway in regulating abundance of the cyclin-dependent kinase inhibitor p27. *Science 269,* 682–685.

(11) Vlach, J., Hennecke, S., and Amati, B. (1997) Phosphorylation-dependent degradation of the cyclin-dependent kinase inhibitor p27. *EMBO J. 16,* 5334–5344.

(12) Kotoshiba, S., Kamura, T., Hara, T., Ishida, N., and Nakayama, K. I. (2005) Molecular dissection of the interaction between p27 and kip1 ubiquitylation-promoting complex, the ubiquitin ligase that regulates proteolysis of p27 in G_1 phase. *J. Biol. Chem. 280,* 17694–17700.

(13) Smith, D. J., Query, C. C., and Konarska, M. M. (2008) Nought may endure but mutability: spliceosome dynamics and the regulated of splicing. *Mol. Cell 30,* 657–666.

(14) van Alphen, R., Wiemer, E., Burger, H., and Eskens, F. (2009) The spliceosome as target for anticancer treatment. *Br. J. Cancer 100,* 228–232.

(15) Will, C. L., Urlaub, H., Achsel, T., Gentzel, M., Wilm, M., and Luhrmann, R. (2002) Characterization of novel SF3b abd 17S U2 snRNP proteins, including a human Prp5p homologue and SF3b DEAD-box protein. *EMBO J. 21,* 4978–4988.

(16) Kotake, Y., Sagane, K., Owa, T., Mimori-Kiyosue, Y., Shimizu, H., Uesugi, M., Ishihama, Y., Iwata, M., and Mizui, Y. (2007) Splicing factor SF3b as a target of the antitumor natural product pladienolide. *Nat. Chem. Biol. 3,* 570–575.

(17) Gozani, O., Potashkin, J., and Reed, R. (1998) A potential role for U2AF-SAP 155 interactions in recruiting U2 snRNP to the branch site. *Mol. Cell. Biol. 18,* 4752–4760.

(18) Will, C. L., Schneider, C., MacMillan, A. M., Katopodis, N. F., Neubauer, G., Wilm, M., Lührmann, R., and Query, C. C. (2001) A novel U2 and U11/U12 snRNP protein that associates with the pre-mRNA branch site. *EMBO J. 20,* 4536–4546.

(19) Tanuma, N., Kim, S. E., Beullens, M., Tsubaki, Y., Mitsuhashi, S., Nomura, M., Kawamura, T., Isono, K., Koseki, H., Sato, M., Bollen, M., Kikuchi, K., and Shima, H. (2008) Nuclear inhibitor of protein phosphatase-1 (NIPP1) directs protein phosphatase-1 (PP1) to dephosphorylate the U2 small nuclear ribonucleoprotein particle (snRNP) component, spliceosome-associated protein 155 (Sap155). *J. Biol. Chem. 283,* 35805–35814.

dx.doi.org/10.1021/cb100248e |*ACS Chem. Biol.* 2011, 6, 229–233